

MATHEMATICAL MODEL FOR 3D FEATURE EXTRACTION FROM MULTIPLE SATELLITE IMAGES DESCRIBED BY RPCs

Jacek Grodecki, Manager, Photogrammetric Systems Engineering
Gene Dial, Director of Product Engineering
James Lutes, Geodetic System Specialist
Space Imaging
12076 Grant Street, Thornton, CO 80241
jgrodecki@spaceimaging.com

ABSTRACT

Rational Polynomial Camera (RPC) models have become the replacement model of choice for a number of high-resolution satellite imagery providers. RPCs provide a simple, efficient, and accurate representation of the camera object-image geometry and allow the end user to perform full photogrammetric processing of satellite imagery including block adjustment, 3D feature extraction and orthorectification. The paper presents a detailed algorithm for estimating 3D object coordinates from multiple overlapping satellite images described by RPCs. The presented algorithm includes, among others, linearization of observation equations, alternative methods for calculating approximate object coordinates, and accuracy analysis methodology. The influence of such factors as convergence angles and physical correlation between images on the accuracy of the estimated object coordinates is then evaluated for a number of different imaging scenarios.

INTRODUCTION

Over the past few years the Rational Polynomial Camera (RPC) models have gained considerable popularity. RPCs provide a generic representation of the camera object-image geometry and yet are simple, efficient, and accurate. It has been demonstrated by (Grodecki, 2001; Grodecki and Dial, 2003; Tao and Hu, 2001 and 2002; Fraser and Hanley, 2003) that RPCs provide the end user of the high-resolution satellite imagery with the ability to perform full photogrammetric processing including block adjustment, 3D feature extraction and orthorectification.

Despite their simplicity, physical interpretation of RPCs is not easy as they provide only a mathematical abstraction of the more complicated physical camera model. The objective of this paper is not only to provide detailed mathematical models for 3D feature extraction with RPCs, but also some physical interpretation of the RPCs sensor geometry.

IKONOS RPC MODEL

IKONOS RPCs, comprising 78 rational polynomial coefficients, $\{c_1...c_{20}, d_1...d_{20}, e_1...e_{20}, f_1...f_{20}\}$ alongside 10 scale and offset factors, are provided by Space Imaging with Geo Ortho Kit and stereo image products. They are generated in the Space Imaging ground station by fitting the RPCs to the physical camera model. The RPC functional model is a ratio of two cubic polynomials of object space coordinates, and as such provides a functional relationship between the object space (ϕ, λ, h) coordinates and the image space (L, S) coordinates. Separate rational functions are provided for mapping the object space coordinates to line and sample coordinates, respectively. To improve numerical precision, image and object space coordinates are normalized to $\langle -1, +1 \rangle$ range by applying the offsets and the scale factors as shown below:

$$U = \frac{\phi - \phi_o}{\phi_s}, V = \frac{\lambda - \lambda_o}{\lambda_s}, W = \frac{h - h_o}{h_s}, X = \frac{S - S_o}{S_s} \text{ and } Y = \frac{L - L_o}{L_s} \quad (1)$$

where ϕ is geodetic latitude, λ is geodetic longitude, h is height above the ellipsoid, S and L are the image sample and line coordinates, and $\phi_o, \lambda_o, h_o, S_o, L_o, \phi_s, \lambda_s, h_s, S_s, L_s$ are the latitude, longitude, height, sample and line offsets and scale factors.

The line and sample rational functions are given in e.g. (Grodecki and Dial, 2003) as:

ASPRS Annual Conference Proceedings
May 2004 * Denver, Colorado
ASPRS – 70 years of service to the profession

$$Y = \frac{N_L(U, V, W)}{D_L(U, V, W)} = \frac{\mathbf{c}^T \mathbf{u}}{\mathbf{d}^T \mathbf{u}}, \text{ and } X = \frac{N_S(U, V, W)}{D_S(U, V, W)} = \frac{\mathbf{e}^T \mathbf{u}}{\mathbf{f}^T \mathbf{u}} \quad (2)$$

where

$$N_L(U, V, W) = c_1 + c_2V + c_3U + c_4W + c_5VU + c_6VW + c_7UW + c_8V^2 + c_9U^2 + c_{10}W^2 + c_{11}UVW + c_{12}V^3 + c_{13}VU^2 + c_{14}VW^2 + c_{15}V^2U + c_{16}U^3 + c_{17}UW^2 + c_{18}V^2W + c_{19}U^2W + c_{20}W^3 = \mathbf{c}^T \mathbf{u}$$

$$D_L(U, V, W) = 1 + d_2V + d_3U + d_4W + d_5VU + d_6VW + d_7UW + d_8V^2 + d_9U^2 + d_{10}W^2 + d_{11}UVW + d_{12}V^3 + d_{13}VU^2 + d_{14}VW^2 + d_{15}V^2U + d_{16}U^3 + d_{17}UW^2 + d_{18}V^2W + d_{19}U^2W + d_{20}W^3 = \mathbf{d}^T \mathbf{u}$$

$$N_S(U, V, W) = e_1 + e_2V + e_3U + e_4W + e_5VU + e_6VW + e_7UW + e_8V^2 + e_9U^2 + e_{10}W^2 + e_{11}UVW + e_{12}V^3 + e_{13}VU^2 + e_{14}VW^2 + e_{15}V^2U + e_{16}U^3 + e_{17}UW^2 + e_{18}V^2W + e_{19}U^2W + e_{20}W^3 = \mathbf{e}^T \mathbf{u}$$

$$D_S(U, V, W) = 1 + f_2V + f_3U + f_4W + f_5VU + f_6VW + f_7UW + f_8V^2 + f_9U^2 + f_{10}W^2 + f_{11}UVW + f_{12}V^3 + f_{13}VU^2 + f_{14}VW^2 + f_{15}V^2U + f_{16}U^3 + f_{17}UW^2 + f_{18}V^2W + f_{19}U^2W + f_{20}W^3 = \mathbf{f}^T \mathbf{u}$$

with

$$\mathbf{u} = [1 \ V \ U \ W \ VU \ VW \ UW \ V^2 \ U^2 \ W^2 \ UVW \ V^3 \ VU^2 \ VW^2 \ V^2U \ U^3 \ UW^2 \ V^2W \ U^2W \ W^3]^T$$

$$\mathbf{c} = [c_1 \ c_2 \ \dots \ c_{20}]^T, \ \mathbf{d} = [d_1 \ d_2 \ \dots \ d_{20}]^T, \ \mathbf{e} = [e_1 \ e_2 \ \dots \ e_{20}]^T, \ \text{and } \mathbf{f} = [f_1 \ f_2 \ \dots \ f_{20}]^T.$$

IKONOS RPC Accuracy

Accuracy of the IKONOS RPC model was analyzed in (Grodecki, 2001) and (Grodecki and Dial, 2001). RPCs were fitted to a grid of points generated using the IKONOS physical camera model and independent checkpoints were used to quantify the RPC model accuracy, for a series of imaging scenarios. The imaging parameters ranged from 0° to 30° for roll, 0° to 30° for pitch, 0° to 360° for scan azimuth, 0° to 60° for latitude, and the strip length was set to 100 km. The checkpoint residual errors were reported to be less than 0.01 pixels RMS and 0.04 pixels worst case for all imaging scenarios, thus demonstrating extremely high accuracy of the RPC camera model representation.

Lutes (2004) verified IKONOS RPC accuracy for a number of different IKONOS image strips up to 70 km in length and reported similar magnitudes of residual and RMS errors to those given in (Grodecki, 2001).

IKONOS RPC accuracy has also been verified empirically against various test ranges by Grodecki and Dial (2002), Ager (2003), and Fraser and Hanley (2004).

3D RECONSTRUCTION ALGORITHMS

3D Reconstruction with Forward RPCs

The Rational Polynomial Camera model given in equation (2) is often referred to as the “Forward” RPC model (Tao and Hu, 2002). The Forward RPC model provides a mapping from object space (ϕ, λ, h) coordinates and the image space (L, S) coordinates. Denormalizing RPCs of eqn. (2) one gets:

$$L = p(\phi, \lambda, h), \text{ and } S = r(\phi, \lambda, h) \quad (3)$$

where

ϕ, λ, h are the geodetic latitude, longitude, and ellipsoidal height,

L, S are the image line and sample coordinates, and

p, r are denormalized RPC models of eqn. (2),

$$p(\phi, \lambda, h) = \frac{N_L(U, V, W)}{D_L(U, V, W)} L_s + L_o, \text{ and } r(\phi, \lambda, h) = \frac{N_S(U, V, W)}{D_S(U, V, W)} S_s + S_o$$

Applying Taylor series expansion one gets the linearized RPC equations at ϕ_o, λ_o, h_o as follows:

$$L = p(\phi_o, \lambda_o, h_o) + \left[\frac{\partial p}{\partial \mathbf{z}^T} \Big|_{\mathbf{z}=\mathbf{z}_o} \right] d\mathbf{z}, \quad S = r(\phi_o, \lambda_o, h_o) + \left[\frac{\partial r}{\partial \mathbf{z}^T} \Big|_{\mathbf{z}=\mathbf{z}_o} \right] d\mathbf{z} \quad (4)$$

where $\frac{\partial p}{\partial \mathbf{z}^T} = \frac{\partial p}{\partial \mathbf{u}^T} \frac{\partial \mathbf{u}}{\partial \mathbf{y}^T} \frac{\partial \mathbf{y}}{\partial \mathbf{z}^T}$, and $\frac{\partial r}{\partial \mathbf{z}^T} = \frac{\partial r}{\partial \mathbf{u}^T} \frac{\partial \mathbf{u}}{\partial \mathbf{y}^T} \frac{\partial \mathbf{y}}{\partial \mathbf{z}^T}$

with

$$\mathbf{u} = [1 \ V \ U \ W \ VU \ VW \ UW \ V^2 \ U^2 \ W^2 \ UVW \ V^3 \ VU^2 \ VW^2 \ V^2U \ U^3 \ UW^2 \ V^2W \ U^2W \ W^3]^T,$$

$$\mathbf{y} = [U \ V \ W]^T, \quad \mathbf{z} = [\phi \ \lambda \ h]^T$$

The partial derivatives are calculated as

$$\frac{\partial p}{\partial \mathbf{u}^T} = \frac{(\mathbf{d}^T \mathbf{u}) \mathbf{c}^T - (\mathbf{c}^T \mathbf{u}) \mathbf{d}^T}{(\mathbf{d}^T \mathbf{u})^2} L_s, \quad \frac{\partial r}{\partial \mathbf{u}^T} = \frac{(\mathbf{f}^T \mathbf{u}) \mathbf{e}^T - (\mathbf{e}^T \mathbf{u}) \mathbf{f}^T}{(\mathbf{f}^T \mathbf{u})^2} S_s, \quad \frac{\partial \mathbf{u}}{\partial \mathbf{y}^T} = \begin{bmatrix} \frac{\partial \mathbf{u}}{\partial U} & \frac{\partial \mathbf{u}}{\partial V} & \frac{\partial \mathbf{u}}{\partial W} \end{bmatrix}$$

with

$$\frac{\partial \mathbf{u}}{\partial U} = [0 \ 0 \ 1 \ 0 \ V \ 0 \ W \ 0 \ 2U \ 0 \ VW \ 0 \ 2VU \ 0 \ V^2 \ 3U^2 \ W^2 \ 0 \ 2UW \ 0]^T$$

$$\frac{\partial \mathbf{u}}{\partial V} = [0 \ 1 \ 0 \ 0 \ U \ W \ 0 \ 2V \ 0 \ 0 \ UW \ 3V^2 \ U^2 \ W^2 \ 2VU \ 0 \ 0 \ 2VW \ 0 \ 0]^T$$

$$\frac{\partial \mathbf{u}}{\partial W} = [0 \ 0 \ 0 \ 1 \ 0 \ V \ U \ 0 \ 0 \ 2W \ UV \ 0 \ 0 \ 2VW \ 0 \ 0 \ 2UW \ V^2 \ U^2 \ 3W^2]^T$$

and

$$\frac{\partial \mathbf{y}}{\partial \mathbf{z}^T} = \begin{bmatrix} \frac{\partial \mathbf{y}}{\partial \phi} & \frac{\partial \mathbf{y}}{\partial \lambda} & \frac{\partial \mathbf{y}}{\partial h} \end{bmatrix}$$

with

$$\frac{\partial \mathbf{y}}{\partial \phi} = \begin{bmatrix} 1 \\ \varphi_s \\ 0 \end{bmatrix}^T, \quad \frac{\partial \mathbf{y}}{\partial \lambda} = \begin{bmatrix} 0 \\ 1 \\ \lambda_s \end{bmatrix}^T, \quad \frac{\partial \mathbf{y}}{\partial h} = \begin{bmatrix} 0 \\ 0 \\ 1 \\ h_s \end{bmatrix}^T.$$

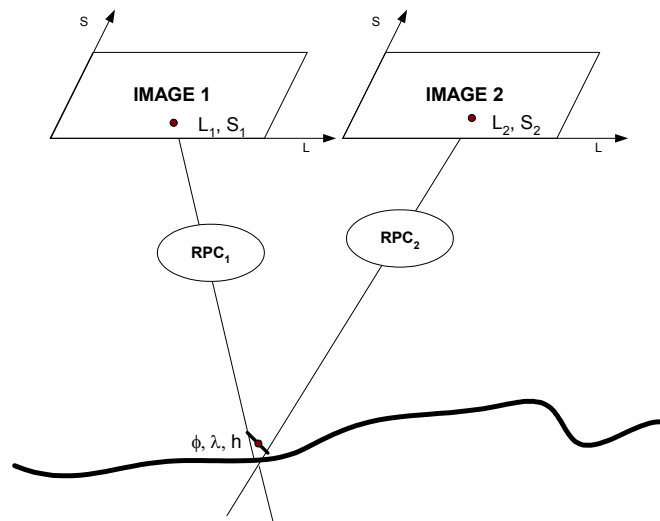


Figure 1. 3D Feature Extraction with RPCs

To estimate object space coordinates of a point one needs to measure its image space coordinates in at least two different images. These images might be part of a same-pass stereo pair or triplet or they might be multiple monoscopic images from different orbital passes. For the case with two images, shown conceptually in Figure 1, the observation equations read:

$$\begin{aligned} L_1 &= p_1(\phi, \lambda, h) + \varepsilon_{L_1} \\ S_1 &= r_1(\phi, \lambda, h) + \varepsilon_{S_1} \\ L_2 &= p_2(\phi, \lambda, h) + \varepsilon_{L_2} \\ S_2 &= r_2(\phi, \lambda, h) + \varepsilon_{S_2} \end{aligned} \quad (5)$$

The linearized observation equations follow with:

$$\mathbf{A}d\mathbf{z} + \boldsymbol{\varepsilon} = \mathbf{w} \text{ with } \mathbf{C}_{\mathbf{w}}, \quad (6)$$

where \mathbf{A} is the first order design matrix, $d\mathbf{z}$ is the vector of corrections to approximate values of object space coordinates, \mathbf{w} is the vector of misclosures, and $\mathbf{C}_{\mathbf{w}}$ its *a priori* covariance matrix,

$$\mathbf{A} = \begin{bmatrix} \left. \frac{\partial p_1}{\partial \mathbf{z}^T} \right|_{\mathbf{z}=\mathbf{z}_0} \\ \left. \frac{\partial r_1}{\partial \mathbf{z}^T} \right|_{\mathbf{z}=\mathbf{z}_0} \\ \left. \frac{\partial p_2}{\partial \mathbf{z}^T} \right|_{\mathbf{z}=\mathbf{z}_0} \\ \left. \frac{\partial r_2}{\partial \mathbf{z}^T} \right|_{\mathbf{z}=\mathbf{z}_0} \end{bmatrix}, \quad d\mathbf{z} = [d\phi \quad d\lambda \quad dh]^T, \quad \text{and } \mathbf{w} = \begin{bmatrix} L_1 \\ S_1 \\ L_2 \\ S_2 \end{bmatrix} - \begin{bmatrix} p_1(\phi_0, \lambda_0, h_0) \\ r_1(\phi_0, \lambda_0, h_0) \\ p_2(\phi_0, \lambda_0, h_0) \\ r_2(\phi_0, \lambda_0, h_0) \end{bmatrix}.$$

The unknown object space coordinates are solved for iteratively. At each iteration step, application of the least-squares principle results in the following estimated corrections to the approximate object space coordinates:

$$d\hat{\mathbf{z}} = \left(\mathbf{A}^T \mathbf{C}_{\mathbf{w}}^{-1} \mathbf{A} \right)^{-1} \mathbf{A}^T \mathbf{C}_{\mathbf{w}}^{-1} \mathbf{w}. \quad (7)$$

At the subsequent iteration step the vector of approximate model parameters \mathbf{z}_0 is replaced by $\hat{\mathbf{z}}$, where $\hat{\mathbf{z}} = \mathbf{z}_0 + d\hat{\mathbf{z}}$, and the math model is linearized again. The least-squares estimation is repeated until convergence is reached. The covariance matrix of the estimated model parameters follows with:

$$\mathbf{C}_{\hat{\mathbf{z}}} = \left(\mathbf{A}^T \mathbf{C}_{\mathbf{w}}^{-1} \mathbf{A} \right)^{-1}. \quad (8)$$

3D Reconstruction with Error Propagation

Error propagation and accuracy estimation of object coordinates determined from multiple overlapping IKONOS images described by RPC models, for the case when *a posteriori* error covariance for the RPC adjustment model parameters is available, has been described in (Dial and Grodecki, 2002). In this paper we will apply this method to the RPC model with offset parameters and examine the effect of correlation between the stereo images on the accuracy of the estimated object coordinates.

As discussed in (Grodecki and Dial, 2003), IKONOS sensor model errors can be accurately characterized by two offset parameters in image space for image strips up to 50 km in length. For longer strips additional drift parameters can be added to model gyro drift errors (Grodecki and Dial, 2003). The RPC model with adjustable offset parameters reads:

$$\begin{aligned} L &= p(\phi, \lambda, h) + a + \varepsilon_L \\ S &= r(\phi, \lambda, h) + b + \varepsilon_S \end{aligned} \quad (9)$$

where

ϕ, λ, h are the geodetic latitude, longitude, and ellipsoidal height,

L, S are the measured image line and sample coordinates,
 p, r are denormalized RPC models (cf. eqn. (3)),
 a, b are the adjustable offset parameters for line and sample, and
 $\varepsilon_L, \varepsilon_S$ are the random unobservable line and sample errors.

As shown in (Dial and Grodecki, 2004), because of high correlation between the attitude and ephemeris errors for narrow field of view cameras such as IKONOS, the offset parameters (a_o, b_o) account for bias errors in both the satellite attitude and the satellite ephemeris.

For the case when the object coordinates are estimated from image coordinate measurements on two overlapping images the observation equations read:

$$\begin{aligned} L_1 &= p_1(\phi, \lambda, h) + a_1 + \varepsilon_{L_1} \\ S_1 &= r_1(\phi, \lambda, h) + b_1 + \varepsilon_{S_1} \\ L_2 &= p_2(\phi, \lambda, h) + a_2 + \varepsilon_{L_2} \\ S_2 &= r_2(\phi, \lambda, h) + b_2 + \varepsilon_{S_2} \end{aligned} \quad (10)$$

The linearized observation equations follow with:

$$\mathbf{A}d\mathbf{x} + \boldsymbol{\varepsilon} = \mathbf{w} \text{ with } \mathbf{C}_w, \quad (11)$$

where \mathbf{A} is the first order design matrix, $d\mathbf{x}$ is the vector of corrections to the initial values of object space coordinates and offset parameters, \mathbf{w} is the vector of misclosures, and \mathbf{C}_w its *a priori* covariance matrix, \mathbf{A} is the first order design matrix, and \mathbf{x} is the vector of block adjustment model parameters,

$$\mathbf{A} = \begin{bmatrix} \mathbf{A}_I & \mathbf{A}_G \\ \mathbf{I} & \mathbf{0} \\ \mathbf{0} & \mathbf{I} \end{bmatrix} \quad d\mathbf{x} = \begin{bmatrix} d\mathbf{x}_I \\ d\mathbf{x}_G \end{bmatrix}$$

where the subscripts **I** and **G** represent image offset parameters and ground coordinates, respectively.

\mathbf{w} is the vector of misclosures and \mathbf{C}_w its *a priori* covariance matrix,

$$\mathbf{w} = \begin{bmatrix} \mathbf{w}_P \\ \mathbf{w}_I \\ \mathbf{w}_G \end{bmatrix} \quad \mathbf{C}_w = \begin{bmatrix} \mathbf{C}_P & \mathbf{0} & \mathbf{0} \\ \mathbf{0} & \mathbf{C}_I & \mathbf{0} \\ \mathbf{0} & \mathbf{0} & \mathbf{C}_G \end{bmatrix}$$

where the subscript **P** represents image space coordinates. \mathbf{C}_P is the *a priori* covariance matrix for image space coordinates. \mathbf{C}_I is the *a priori* covariance matrix for image offset parameters resulting from the preceding block adjustment of the images. If the block adjustment results are not available then manufacturer specified accuracies and correlations should be used to construct \mathbf{C}_I . \mathbf{C}_G is the *a priori* covariance matrix for ground coordinates.

$$\mathbf{A}_I = \mathbf{I}_{4 \times 4}, \quad \mathbf{A}_G = \begin{bmatrix} \left. \frac{\partial p_1}{\partial \mathbf{z}^T} \right|_{\mathbf{z}=\mathbf{z}_o} \\ \left. \frac{\partial r_1}{\partial \mathbf{z}^T} \right|_{\mathbf{z}=\mathbf{z}_o} \\ \left. \frac{\partial p_2}{\partial \mathbf{z}^T} \right|_{\mathbf{z}=\mathbf{z}_o} \\ \left. \frac{\partial r_2}{\partial \mathbf{z}^T} \right|_{\mathbf{z}=\mathbf{z}_o} \end{bmatrix}, \quad d\mathbf{x}_I = [da_1 \quad db_1 \quad da_2 \quad db_2]^T, \quad d\mathbf{x}_G = d\mathbf{z}, \quad \text{and } \mathbf{w} = \begin{bmatrix} L_1 \\ S_1 \\ L_2 \\ S_2 \end{bmatrix} - \begin{bmatrix} p_1(\phi_o, \lambda_o, h_o) + a_{10} \\ r_1(\phi_o, \lambda_o, h_o) + b_{10} \\ p_2(\phi_o, \lambda_o, h_o) + a_{20} \\ r_2(\phi_o, \lambda_o, h_o) + b_{20} \end{bmatrix}.$$

Initial values of the offset parameters should be set to zero, if the block adjustment estimates were used to update the RPC model, as is the case with the IKONOS stereo images. Otherwise, they should be set to the values resulting from the block adjustment.

As before, an iterative process is used to solve for the vector of model parameters. At each iteration step, application of the least-squares principle results in the following estimated corrections to the approximate object space coordinates

$$d\hat{\mathbf{x}} = (\mathbf{A}^T \mathbf{C}_w^{-1} \mathbf{A})^{-1} \mathbf{A}^T \mathbf{C}_w^{-1} \mathbf{w}, \quad (12)$$

with the covariance matrix of the estimated model parameters given as

$$\mathbf{C}_{\hat{\mathbf{x}}} = (\mathbf{A}^T \mathbf{C}_w^{-1} \mathbf{A})^{-1}. \quad (13)$$

The 3×3 submatrix corresponding to the object space coordinates can then be extracted from the full covariance matrix $\mathbf{C}_{\hat{\mathbf{x}}}$ and used for calculating the elements of the *a posteriori* error ellipsoid for the given object point.

To take into account correlation between the two images comprising the stereo pair one could either use a fully populated image offset covariance matrix \mathbf{C}_1 or add common bias terms to the observation equations. Common bias terms provide an intuitive way to quantify errors common to the two images of a stereo pair. The observation equations of a model with common bias terms a_B and b_B read:

$$\begin{aligned} L_1 &= p_1(\phi, \lambda, h) + a_{R1} + a_B + \varepsilon_{L_1} \\ S_1 &= r_1(\phi, \lambda, h) + b_{R1} + b_B + \varepsilon_{S_1} \\ L_2 &= p_2(\phi, \lambda, h) + a_{R2} + a_B + \varepsilon_{L_2} \\ S_2 &= r_2(\phi, \lambda, h) + b_{R2} + b_B + \varepsilon_{S_2} \end{aligned} \quad (14)$$

The linearized observation equations read:

$$\mathbf{A}d\mathbf{x} + \boldsymbol{\varepsilon} = \mathbf{w} \text{ with } \mathbf{C}_w, \quad (15)$$

with

$$\mathbf{A} = \begin{bmatrix} \mathbf{A}_{\mathbf{I}_B} & \mathbf{A}_{\mathbf{G}} \\ \mathbf{I} & \mathbf{0} \\ \mathbf{0} & \mathbf{I} \end{bmatrix}, \quad d\mathbf{x} = \begin{bmatrix} d\mathbf{x}_{\mathbf{I}_B} \\ d\mathbf{x}_{\mathbf{G}} \end{bmatrix}, \quad \mathbf{A}_{\mathbf{I}_B} = \begin{bmatrix} 1 & 0 & 0 & 0 & 1 & 0 \\ 0 & 1 & 0 & 0 & 0 & 1 \\ 0 & 0 & 1 & 0 & 1 & 0 \\ 0 & 0 & 0 & 1 & 0 & 1 \end{bmatrix},$$

where the subscripts \mathbf{I}_B and \mathbf{G} represent image offset parameters and ground coordinates, respectively.

The vector of misclosures and its *a priori* covariance matrix, read:

$$\mathbf{w} = \begin{bmatrix} \mathbf{w}_P \\ \mathbf{w}_{\mathbf{I}_B} \\ \mathbf{w}_{\mathbf{G}} \end{bmatrix}, \quad \text{and } \mathbf{C}_w = \begin{bmatrix} \mathbf{C}_P & \mathbf{0} & \mathbf{0} \\ \mathbf{0} & \mathbf{C}_{\mathbf{I}_B} & \mathbf{0} \\ \mathbf{0} & \mathbf{0} & \mathbf{C}_{\mathbf{G}} \end{bmatrix},$$

where the *a priori* covariance matrix for image offset parameters $\mathbf{C}_{\mathbf{I}_B}$ is a block diagonal matrix given as:

$$\mathbf{C}_{\mathbf{I}_B} = \begin{bmatrix} C_{a_{R1}a_{R1}} & C_{a_{R1}b_{R1}} & 0 & 0 & 0 & 0 \\ C_{b_{R1}a_{R1}} & C_{b_{R1}b_{R1}} & 0 & 0 & 0 & 0 \\ 0 & 0 & C_{a_{R2}a_{R2}} & C_{a_{R2}b_{R2}} & 0 & 0 \\ 0 & 0 & C_{b_{R2}a_{R2}} & C_{b_{R2}b_{R2}} & 0 & 0 \\ 0 & 0 & 0 & 0 & C_{a_B a_B} & 0 \\ 0 & 0 & 0 & 0 & 0 & C_{b_B b_B} \end{bmatrix}$$

The vector of image offset parameters and the vector of misclosures are given as:

$$d\mathbf{x}_{\mathbf{I}_B} = [da_{R1} \quad db_{R1} \quad da_{R2} \quad db_{R2} \quad da_B \quad db_B]^T, \quad (16)$$

$$\mathbf{w} = \begin{bmatrix} L_1 \\ S_1 \\ L_2 \\ S_2 \end{bmatrix} - \begin{bmatrix} p_1(\phi_o, \lambda_o, h_o) + a_{R1_0} + a_B \\ r_1(\phi_o, \lambda_o, h_o) + b_{R1_0} + b_B \\ p_2(\phi_o, \lambda_o, h_o) + a_{R2_0} + a_B \\ r_2(\phi_o, \lambda_o, h_o) + b_{R2_0} + b_B \end{bmatrix}. \quad (17)$$

We will now show that the model with common bias terms is equivalent to the model of eqn. (11) with a fully populated *a priori* covariance matrix \mathbf{C}_I . The image offset parameters of the two models and their *a priori* covariance matrices are functionally related as follows:

$$\begin{bmatrix} da_1 \\ db_1 \\ da_2 \\ db_2 \end{bmatrix} = \mathbf{J} \begin{bmatrix} da_{R1} \\ db_{R1} \\ da_{R2} \\ db_{R2} \\ da_B \\ db_B \end{bmatrix} \quad \text{where } \mathbf{J} = \begin{bmatrix} 1 & 0 & 0 & 0 & 1 & 0 \\ 0 & 1 & 0 & 0 & 0 & 1 \\ 0 & 0 & 1 & 0 & 1 & 0 \\ 0 & 0 & 0 & 1 & 0 & 1 \end{bmatrix}, \quad (18)$$

and:

$$\mathbf{C}_I = \mathbf{J} \mathbf{C}_{IB} \mathbf{J}^T = \begin{bmatrix} C_{a_{R1}a_{R1}} + C_{a_Ba_B} & C_{a_{R1}b_{R1}} & C_{a_Ba_B} & 0 \\ C_{b_{R1}a_{R1}} & C_{b_{R1}b_{R1}} + C_{b_Bb_B} & 0 & C_{b_Bb_B} \\ C_{a_Ba_B} & 0 & C_{a_{R2}a_{R2}} + C_{a_Ba_B} & C_{a_{R2}b_{R2}} \\ 0 & C_{b_Bb_B} & C_{b_{R2}a_{R2}} & C_{b_{R2}b_{R2}} + C_{b_Bb_B} \end{bmatrix}$$

Thus the following relationship exists between the common bias parameters and the image-to-image correlation coefficients:

$$\rho_L = \frac{C_{a_Ba_B}}{\sqrt{(C_{a_{R1}a_{R1}} + C_{a_Ba_B})(C_{a_{R2}a_{R2}} + C_{a_Ba_B})}}, \quad \text{and} \quad \rho_S = \frac{C_{b_Bb_B}}{\sqrt{(C_{b_{R1}b_{R1}} + C_{b_Bb_B})(C_{b_{R2}b_{R2}} + C_{b_Bb_B})}}, \quad (19)$$

where ρ_L and ρ_S are the correlation coefficients between line coordinates of image 1 and image 2, and between sample coordinates of image 1 and image 2, respectively.

Calculation of Approximate Ground Coordinates

3D reconstruction with the Forward RPC model requires knowledge of the approximate object space coordinates. Tao and Hu (2002) proposed to use the truncated RPCs, i.e. RPCs with only the first-order terms, to this end. In order for the truncated RPCs to provide a reasonably accurate solution, the higher order RPC terms have to be negligibly small. Unfortunately this is often not the case with the IKONOS RPCs; oftentimes neglecting higher order terms results in hundreds of meters of error. Accuracy of the truncated RPCs can be easily checked by comparing the line and sample coordinates calculated with the truncated RPCs against the line and sample coordinates calculated with the original RPCs over the entire RPC range, i.e. $\varphi_o \pm \varphi_s$, $\lambda_o \pm \lambda_s$ and $h_o \pm h_s$. If the truncated RPCs are determined not to be accurate enough, DLTs fitted to the original RPC model can be used to determine the approximate ground coordinates of the object point. The DLT fitting process is in principle identical to the RPC fitting process, description of which can be found in (Tao and Hu, 2001). An algorithm for determining the object space coordinates with the truncated RPCs is given in (Tao and Hu, 2002). Since the DLT functional model is essentially identical to the truncated RPC model, the same algorithm can be applied to the DLT case.

Other possibilities for calculating the approximate object space coordinates include application of the Inverse RPC model (Tao and Hu, 2002) or using the results of the first iteration in the Straight Line algorithm given in the “3D Reconstruction Using Straight Line Algorithm” section below.

3D Reconstruction with Inverse RPCs

The “Inverse” RPC model (Tao and Hu, 2002) provides a mapping from image space (L, S) coordinates at a given height h , to object space (ϕ, λ) coordinates. Inverse RPC model can be generated from the Forward RPC model. This can be done by fitting Inverse RPCs to a 3D grid of points generated with the Forward RPC model, using e.g. an algorithm described in (Tao and Hu, 2001). An algorithm for 3D reconstruction with the Inverse RPC model is given in (Tao and Hu, 2002).

3D Reconstruction Using Straight Line Algorithm

3D reconstruction can also be performed by approximating progressively smaller segments of the image-to-ground rays by straight lines as follows. Given two overlapping images described by RPCs, the first step is to determine the approximate height range for the 3D intersection of the two rays. The approximate min and max heights can be calculated as

$$h_{max} = \max(h_{max1}, h_{max2}) \text{ and } h_{min} = \min(h_{min1}, h_{min2}), \quad (20)$$

with

$$h_{max1} = h_{o1} + h_{s1}, \quad h_{min1} = h_{o1} - h_{s1}, \quad h_{max2} = h_{o2} + h_{s2}, \quad h_{min2} = h_{o2} - h_{s2},$$

where h_{o1} , h_{s1} and h_{o2} , h_{s2} are the RPC height offsets and scale factors for image 1 and 2, respectively.

With (L_1, S_1) and (L_2, S_2) being the measured image space coordinates on image 1 and 2, respectively, the next step is to calculate the object space coordinates $(\phi_{max1}, \lambda_{max1})$, $(\phi_{min1}, \lambda_{min1})$, $(\phi_{max2}, \lambda_{max2})$, $(\phi_{min2}, \lambda_{min2})$ of the intersection points of each of the two image rays with the h_{max} and h_{min} height surfaces using the image-to-ground RPC algorithm described below. The so determined min / max pairs of object space points are then used to calculate equations of straight lines in ECF coordinate system, approximating the two image rays:

$$\begin{cases} X = X_{min1} + t_1(X_{max1} - X_{min1}) \\ Y = Y_{min1} + t_1(Y_{max1} - Y_{min1}) \\ Z = Z_{min1} + t_1(Z_{max1} - Z_{min1}) \end{cases} \quad (21)$$

and

$$\begin{cases} X = X_{min2} + t_2(X_{max2} - X_{min2}) \\ Y = Y_{min2} + t_2(Y_{max2} - Y_{min2}) \\ Z = Z_{min2} + t_2(Z_{max2} - Z_{min2}) \end{cases} \quad (22)$$

where

$$\begin{aligned} X_i &= [N(\varphi_i) + h_i] \cos \varphi_i \cos \lambda_i \\ Y_i &= [N(\varphi_i) + h_i] \cos \varphi_i \sin \lambda_i \\ Z_i &= [N(\varphi_i)(1 - e^2) + h_i] \sin \varphi_i \end{aligned} \quad (23)$$

The intersection of these two lines can be determined by calculating a least-squares estimate of X , Y , Z , t_1 and t_2 . Given the so calculated intersection point, the solution can be further refined by setting new min / max heights close to the previously calculated height of the intersection point, and repeating the entire process. If needed, the estimation process can be iterated further.

Image-to-Ground RPC Algorithm

Given approximate object space coordinates (ϕ_o, λ_o) and measured image space coordinates (L, S) of a point, the task is to calculate its object space coordinates (ϕ, λ) at a fixed height h_f for an image described by the RPC model of eqn. (3). Rearranging the line and sample RPC equations we get:

$$\begin{aligned} f(\mathbf{v}) &= p(\phi, \lambda, h_f) - L = \frac{N_L(U, V, W_f)}{D_L(U, V, W_f)} L_s + L_o - L = 0 \\ g(\mathbf{v}) &= r(\phi, \lambda, h_f) - S = \frac{N_S(U, V, W_f)}{D_S(U, V, W_f)} S_s + S_o - S = 0 \end{aligned} \quad (24)$$

or

$$\mathbf{F}(\mathbf{v}) = \begin{bmatrix} f(\mathbf{v}) \\ g(\mathbf{v}) \end{bmatrix} = \mathbf{0}$$

where $\mathbf{v} = [U \ V]^T$.

To calculate corrections to the approximate object space coordinates (ϕ_o, λ_o) one can use the Newton-Raphson method as follows:

$$d\mathbf{v}_i = -[\mathbf{J}(\mathbf{v}_i)]^{-1} \mathbf{F}(\mathbf{v}_i) \quad (25)$$

where

$$\mathbf{v}_i = \mathbf{v}_{i-1} + d\mathbf{v}_{i-1}$$

and

$$\mathbf{v}_o = [U_o \ V_o]^T = \begin{bmatrix} \frac{\phi - \phi_o}{\phi_s} & \frac{\lambda - \lambda_o}{\lambda_s} \end{bmatrix}^T.$$

The Jacobian matrix \mathbf{J} is defined as:

$$\mathbf{J}(\mathbf{v}) = \begin{bmatrix} \frac{\partial f}{\partial U} & \frac{\partial f}{\partial V} \\ \frac{\partial g}{\partial U} & \frac{\partial g}{\partial V} \end{bmatrix} \quad (26)$$

where $\frac{\partial f}{\partial U} = \frac{\partial f}{\partial \mathbf{u}^T} \frac{\partial \mathbf{u}}{\partial U}$, $\frac{\partial f}{\partial V} = \frac{\partial f}{\partial \mathbf{u}^T} \frac{\partial \mathbf{u}}{\partial V}$, $\frac{\partial g}{\partial U} = \frac{\partial g}{\partial \mathbf{u}^T} \frac{\partial \mathbf{u}}{\partial U}$, and $\frac{\partial g}{\partial V} = \frac{\partial g}{\partial \mathbf{u}^T} \frac{\partial \mathbf{u}}{\partial V}$.

The partial derivatives are calculated as

$$\frac{\partial f}{\partial \mathbf{u}^T} = \frac{(\mathbf{d}^T \mathbf{u}) \mathbf{c}^T - (\mathbf{c}^T \mathbf{u}) \mathbf{d}^T}{(\mathbf{d}^T \mathbf{u})^2} L_s$$

$$\frac{\partial g}{\partial \mathbf{u}^T} = \frac{(\mathbf{f}^T \mathbf{u}) \mathbf{e}^T - (\mathbf{e}^T \mathbf{u}) \mathbf{f}^T}{(\mathbf{f}^T \mathbf{u})^2} S_s$$

$$\frac{\partial \mathbf{u}}{\partial U} = \begin{bmatrix} 0 & 0 & 1 & 0 & V & 0 & W & 0 & 2U & 0 & VW & 0 & 2VU & 0 & V^2 & 3U^2 & W^2 & 0 & 2UW & 0 \end{bmatrix}^T$$

$$\frac{\partial \mathbf{u}}{\partial V} = \begin{bmatrix} 0 & 1 & 0 & 0 & U & W & 0 & 2V & 0 & 0 & UW & 3V^2 & U^2 & W^2 & 2VU & 0 & 0 & 2VW & 0 & 0 \end{bmatrix}^T$$

Inverse of the Jacobian matrix \mathbf{J} is finally calculated as

$$[\mathbf{J}(\mathbf{v})]^{-1} = \frac{1}{|\mathbf{J}(\mathbf{v})|} \begin{bmatrix} \frac{\partial g}{\partial V} & -\frac{\partial f}{\partial V} \\ -\frac{\partial g}{\partial U} & \frac{\partial f}{\partial U} \end{bmatrix} \text{ with } |\mathbf{J}(\mathbf{v})| = \frac{\partial f}{\partial U} \frac{\partial g}{\partial V} - \frac{\partial g}{\partial U} \frac{\partial f}{\partial V}. \quad (27)$$

To calculate the approximate object space coordinates (ϕ_o, λ_o) one can use either truncated RPCs, i.e. RPCs with only the first-order terms, or, if truncated RPCs were not accurate enough, DLTs fitted to the original RPC model. In either case the functional model would read:

$$L = \frac{a_0 + a_1 U + a_2 V + a_3 W_f}{1 + b_1 U + b_2 V + b_3 W_f} \quad (28)$$

$$S = \frac{c_0 + c_1 U + c_2 V + c_3 W_f}{1 + d_1 U + d_2 V + d_3 W_f}$$

Multiplying both sides by the denominator we get the following set of equations

$$\begin{aligned} L(1 + b_3 W_f) - a_0 - a_3 W_f &= (a_1 - L b_1) U + (a_2 - L b_2) V \\ S(1 + d_3 W_f) - c_0 - c_3 W_f &= (c_1 - S d_1) U + (c_2 - S d_2) V \end{aligned} \quad (29)$$

or

$$\mathbf{y} = \mathbf{A}\mathbf{v} \quad (30)$$

with

$$\mathbf{y} = \begin{bmatrix} L(1 + b_3 W_f) - a_0 - a_3 W_f \\ S(1 + d_3 W_f) - c_0 - c_3 W_f \end{bmatrix}, \quad \mathbf{A} = \begin{bmatrix} (a_1 - Lb_1) & (a_2 - Lb_2) \\ (c_1 - Sd_1) & (c_2 - Sd_2) \end{bmatrix}, \quad \text{and } \mathbf{v} = [U \ V]^T.$$

The solution for \mathbf{v} follows with

$$\mathbf{v} = \mathbf{A}^{-1}\mathbf{y} \quad (31)$$

where

$$\mathbf{A}^{-1} = \frac{1}{|\mathbf{A}|} \begin{bmatrix} (c_2 - Sd_2) & (-a_2 + Lb_2) \\ (-c_1 + Sd_1) & (a_1 - Lb_1) \end{bmatrix} \text{ with } |\mathbf{A}| = (a_1 - Lb_1)(c_2 - Sd_2) - (c_1 - Sd_1)(a_2 - Lb_2).$$

NUMERICAL EXAMPLES

Numerical examples illustrating the influence of the convergence angle and the physical correlation between images on the accuracy of the estimated object coordinates are presented in this section.

Influence of the Convergence Angle

It is assumed that the object point coordinates are determined from a symmetric stereo pair, where the two images are collected from opposite collection azimuths and have the same collection elevation angles. The ephemeris accuracy is assumed to be 1 meter (1σ) while the attitude accuracy is specified at 6 μrad . The convergence angle is varied between 10 and 90 degrees. The results are summarized in Figure 2. As expected, it is seen that vertical accuracy drops rapidly as the convergence angle gets smaller. For the 30 to 45 degree convergence angle range typical for IKONOS stereo images the horizontal accuracy is nearly constant at 3.5 m (1σ), while the vertical accuracy ranges from 9 m to 13 m (1σ).

Horizontal and Vertical Accuracy vs. Convergence Angle

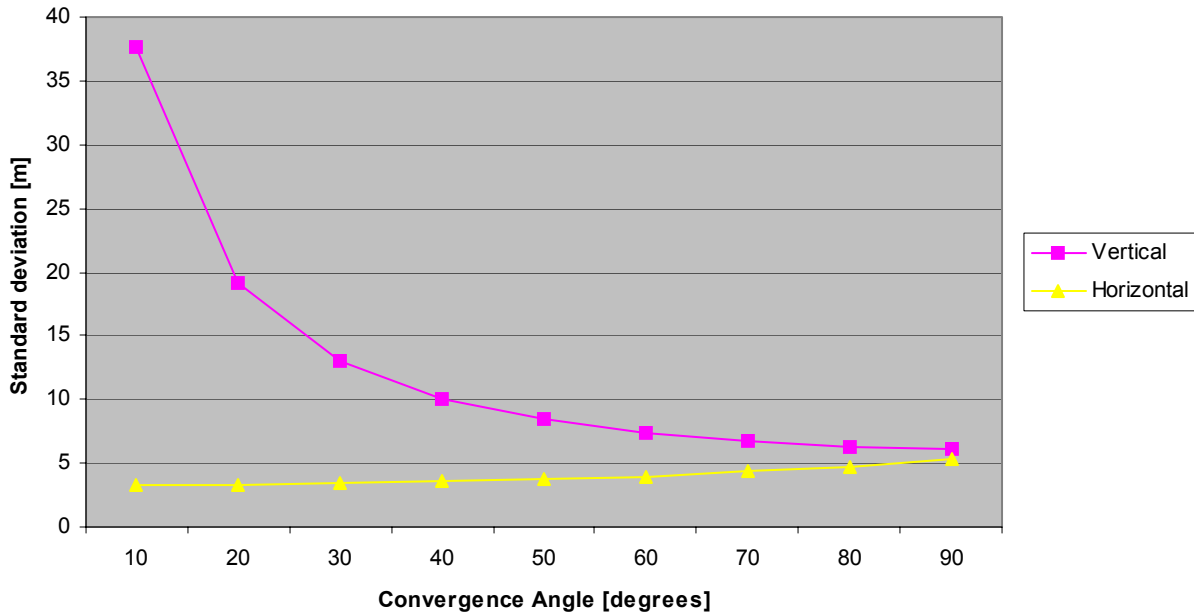


Figure 2. Accuracy vs. Convergence Angle.

Influence of Image-to-Image Correlation

Two cases are analyzed in this section. In the first case it is assumed that the two images comprising the stereo pair are uncorrelated, as would be the case with the cross-track stereo images collected on different orbital passes. In the second case the assumption is that the two images of the stereo pair are significantly correlated. This would happen if both images were collected on the same orbital pass, which is always the case for the IKONOS stereo products. The a priori accuracy of each image is 4 meters (1σ) in line and sample and it is assumed that there is no correlation between line and sample coordinates within each image. For the correlated case the amount of common bias is varied from 1 to 4 meters. The results are summarized in Figure 3.

It is seen that the vertical accuracy improves as the images in the stereo pair become more correlated. There is a slight degradation of the horizontal accuracy as there is progressively less averaging out of the random errors affecting both images as they become more correlated, but this effect is seen not to be very significant. This suggests that same-pass stereo imagery has superior accuracy characteristics over cross-track stereo imagery.

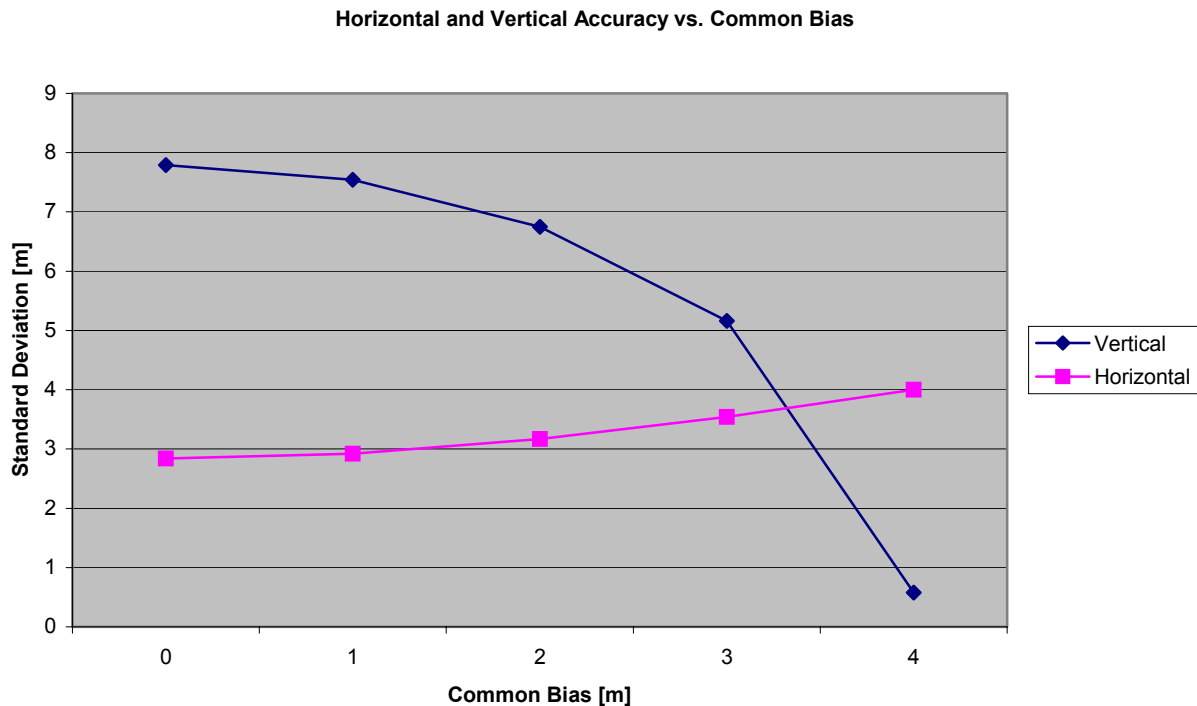


Figure 3. Accuracy vs. Correlation.

CONCLUSIONS

Multiple alternative algorithms for 3D feature extraction using RPCs have been presented. In addition, the influence of convergence angle and physical correlation on 3D feature extraction accuracy has been evaluated for a number of different imaging scenarios. As with any other sensor models, vertical accuracy of 3D feature extraction with RPCs gets worse as the convergence angle gets smaller. It has also been seen that the vertical accuracy improves as the images in the stereo pair become more correlated, thus suggesting that same-pass stereo imagery has superior accuracy characteristics over cross-track stereo imagery.

REFERENCES

- Ager, T.P. (2003). "Evaluation of the geometric accuracy of Ikonos imagery." *SPIE 2003 AeroSense Conference*, Orlando, 21-25 April, 8 pages.
- Dial, Gene and Jacek Grodecki (2002). "IKONOS Accuracy without Ground Control." *Proceedings of ASPRS Commission I Mid-Term Symposium*, Denver, November 10-15, 2002.
- Dial, Gene and Jacek Grodecki (2004). "Satellite Image Block Adjustment Simulations." *Proceedings of ASPRS 2004 Conference*, Denver, May 23-28, 2004.
- Fraser, Clive S. and Harry B. Hanley (2003). "Bias Compensation in Rational Functions for Ikonos Satellite Imagery." *Photogrammetric Engineering & Remote Sensing*, 69(1): 53-57.
- Fraser, Clive S. and Harry B. Hanley (2003). "Bias Compensated RPCs for Sensor Orientation of High-Resolution Satellite Imagery." *Proceedings of ASPRS 2004 Conference*, Denver, May 23-28, 2004.
- Grodecki, Jacek (2001). "IKONOS Stereo Feature Extraction—RPC Approach." *Proceedings of ASPRS 2001 Conference*, St. Louis, April 23-27, 2001.

- Grodecki, Jacek and Gene Dial (2001). "IKONOS Geometric Accuracy." *Proceedings of Joint Workshop of ISPRS Working Groups I/2, I/5 and IV/7 on High Resolution Mapping from Space 2001*, University of Hannover, Hannover, Germany, Sept 19-21, 2001.
- Grodecki, Jacek and Gene Dial (2002). "IKONOS Geometric Accuracy Validation." *Proceedings of ISPRS Commission I Mid-Term Symposium*, Denver, November 10-15, 2002.
- Grodecki, Jacek and Gene Dial (2003). "Block Adjustment of High-Resolution Satellite Images Described by Rational Polynomials." *Photogrammetric Engineering & Remote Sensing*, 69(1): 59-68.
- Grodecki, Jacek, Gene Dial and James Lutes (2003). "Error propagation in block adjustment of high-resolution satellite images." *Proceedings of ASPRS 2003 Conference*, Anchorage, May 5-9, 2003.
- Lutes, James (2004). "Accuracy Analysis of Rational Polynomial Coefficients for IKONOS Imagery." *Proceedings of ASPRS 2004 Conference*, Denver, May 23-28, 2004.
- Tao, C. Vincent and Yong Hu (2001). "A Comprehensive Study of the Rational Function Model for Photogrammetric Processing." *Photogrammetric Engineering & Remote Sensing*, 67(12): 1347-1357.
- Tao, C. Vincent and Yong Hu (2002). "3D Reconstruction of the Rational Function Models for Photogrammetric Processing." *Photogrammetric Engineering & Remote Sensing*, 68(7): 705-714.